

Supporting Information: Ideal charge density wave order in the high-field state of superconducting YBCO

H. Jang^{a,1}, W.-S. Lee^{b,1}, H. Nojiri^c, S. Matsuzawa^c, H. Yasumura^c, L. Nie^d, A. V. Maharaj^d, S. Gerber^e, Y.-J. Liu^a, A. Mehta^a, D. A. Bonn^{f,g}, R. Liang^{f,g}, W. N. Hardy^{f,g}, C. A. Burns^{a,h}, Z. Islamⁱ, S. Song^j, J. Hastings^j, T. P. Devereaux^b, Z.-X. Shen^{b,d}, S. A. Kivelson^d, C.-C. Kao^k, D. Zhu^{i,2}, and J.-S. Lee^{a,1,2}

^aStanford Synchrotron Radiation Lightsource, SLAC National Accelerator Laboratory, Menlo Park, CA 94025; ^bStanford Institute for Materials and Energy Science, SLAC National Accelerator Laboratory and Stanford University, Menlo Park, CA 94025; ^cInstitute for Materials Research, Tohoku University, Katahira 2-1-1, Sendai, 980-8577, Japan; ^dGeballe Laboratory for Advanced Materials, Departments of Physics and Applied Physics, Stanford University, Stanford, CA 94305; ^eSwissFEL, Paul Scherrer Institut, 5232 Villigen PSI, Switzerland; ^fDepartment of Physics & Astronomy, University of British Columbia, Vancouver, British Columbia, Canada V6T 1Z1; ^gCanadian Institute for Advanced Research, Toronto, Ontario, Canada M5G 1Z8; ^hDepartment of Physics, Western Michigan University, Kalamazoo, MI, 49008; ⁱThe Advanced Photon Source, Argonne National Laboratory, Argonne, IL 60439; ^jLinac Coherent Light Source, SLAC National Accelerator Laboratory, Menlo Park, CA 94025; ^kSLAC National Accelerator Laboratory, Menlo Park, CA 94025

This supporting information was compiled on September 27, 2016

Our proposed interpretation of the x-ray results involves two basic assumptions: 1) In the absence of disorder, the intrinsic electronic correlations favor the formation of a unidirectional, incommensurate CDW, and 2) there are large scale inhomogeneities in the sample, which we treat schematically as regions of “More” and “Less” disorder. In this Supporting Information, we discuss how such assumptions can lead naturally to a sharp crossover in the directionality and correlation length of the CDW as the magnetic field is increased. Figure 5 in the main text illustrates the basic physics - in the $\sigma - \Lambda$ plane where σ characterizes the strength of disorder and Λ is the strength of the CDW (an increasing function of increasing magnetic field), there is a sharp crossover from short ranged bidirectional CDW correlations to longer ranged, strongly unidirectional CDW correlations. In a tetragonal cuprate, this would be associated with a thermodynamic phase transition to a nematic state, a form of “vestigial” order. We assume that at low fields both More and Less disordered regions are in the isotropic phase, while at low temperatures above a critical field strength the Less disordered regions enter the nematic phase, thus exhibiting strong unidirectional character.

A classical effective field theory

While many of the major points that underlie our proposal follow on rather general grounds from the statistical mechanics of disordered systems, the most straightforward way to illustrate them is by turning to the solution of the effective model of an incommensurate CDW introduced in Ref. [S1]. We consider a classical effective field theory with two complex fields, $\psi_x(\vec{r})$ and $\psi_y(\vec{r})$, representing the slowly varying amplitude of a CDW at wave vectors $\vec{Q}_x = q\hat{x}$ and $\vec{Q}_y = q\hat{y}$, respectively. A biquadratic coupling of the form $2\Delta|\psi_x|^2|\psi_y|^2$ appears in the effective action, where we take $\Delta > 0$ which favors unidirectional (stripe) over bidirectional (checkerboard) order. This model can be solved in the self-consistent Gaussian approximation using the replica trick to treat the disorder. The results are controlled in a formal $N \rightarrow \infty$ limit in which ψ_x is an $O(N)$ vector; it has been shown to agree qualitatively with results of Monte-Carlo simulations on the same model for the physical ($N = 2$) case in Ref. [S2].

As we are only interested in qualitative results, we will simplify the problem at the expense of neglecting several material specific features of YBCO: We consider a model with

one plane per unit cell and assume an interlayer coupling, $V_z > 0$, that favors in-phase interplane ordering. Moreover, we have not included the in-plane anisotropy of the CDW stiffness constants, *i.e.* in the notation of Ref. [S1] we have taken $\kappa_{\parallel} = \kappa_{\perp} = 1$. (The final equality amounts to a particular choice of units of in-plane length, $b = 1$.)

For this simplified model, (for in-plane momenta $k_x^2 + k_y^2 \ll q^2$) the CDW structure factor can be expressed as

$$\begin{aligned} S(\vec{k} + \vec{Q}_x) &= TG(\vec{k}, \mu + \mathcal{N}) + \sigma^2 |G(\vec{k}, \mu + \mathcal{N})|^2 \\ S(\vec{k} + \vec{Q}_y) &= TG(\vec{k}, \mu - \mathcal{N}) + \sigma^2 |G(\vec{k}, \mu - \mathcal{N})|^2 \end{aligned} \quad [\text{S1}]$$

where

$$G^{-1}(\vec{k}, \mu) = \mu + k_x^2 + k_y^2 + V_z[1 - \cos(k_z c)]. \quad [\text{S2}]$$

G can be recognized as the simple Ornstein Zernike form of the order parameter correlations in a generic system in the disordered phase proximate to a critical point. k_z is the out-of-plane dispersion and c is the c -axis lattice parameter. The only subtlety is that the effective chemical potential (μ) and the “nematic order parameter” (\mathcal{N}), are determined from the self-consistency equations,

$$\Lambda(T, H) = \int \frac{d\vec{k}}{(2\pi)^3} [S(\vec{k} + \vec{Q}_x) + S(\vec{k} + \vec{Q}_y)] \quad [\text{S3}]$$

where Λ is the mean squared amplitude of the CDW order parameter (assumed to be an otherwise known function of T and H), and

$$\mathcal{N} = \mathcal{N}_0 + 2\Delta \int \frac{d\vec{k}}{(2\pi)^3} [S(\vec{k} + \vec{Q}_y) - S(\vec{k} + \vec{Q}_x)] \quad [\text{S4}]$$

where \mathcal{N}_0 is an intrinsic nematicity (due to the orthorhombicity of the crystal). Again, for simplicity, we will henceforth report results in the limit $\mathcal{N}_0 \rightarrow 0^+$. In this case, $\mathcal{N} = 0$ is always a possible solution of the self-consistency equations. However, if the CDW ordering tendency is sufficiently strong (*i.e.* for $\Lambda(T, H) > \Lambda_c$ where the critical value Λ_c is itself a function of

¹These authors (H.J., W.-S.L., and J.-S.L.) contributed equally to this work.

²To whom correspondence should be addressed. E-mail: dzhu@slac.stanford.edu (D.Z.) or jslee@slac.stanford.edu (J.-S.L.)

125 T and σ), a second solution with $\mathcal{N} > 0$ is preferred; this is the
 126 nematic phase which spontaneously breaks the point-group
 127 symmetry. Consistent with general theorems, so long as $\sigma > 0$,
 128 the CDW order inferred from these equations always has a
 129 finite correlation length, *i.e.* there is never long-range CDW
 130 order in the presence of even weak quenched randomness.

131 This set of equations was analyzed under various circum-
 132 stances in Ref. [S1]. Generally, as the system is tuned from
 133 the isotropic to the nematic phase in any fashion (for instance,
 134 by increasing Λ) several changes in the nature of the correla-
 135 tions onset very rapidly at the transition point: The in-plane
 136 correlation length, ξ_{ab} , grows substantially as does the inter-
 137 plane correlation length, ξ_c , so long as V_z is not too small.
 138 The degree of directionality, $S(\vec{Q}_y)/S(\vec{Q}_x)$, which is 1 in the
 139 isotropic phase, becomes rapidly much larger than 1 in the
 140 nematic phase. Simultaneously, the peak intensity, $S(\vec{Q}_y)$,
 141 shows the most dramatic increase of all.

142 As an illustrative example, we consider the simplest case of
 143 $T = 0$ and vanishingly small interplane [S3] coupling, $V_z \rightarrow 0$.
 144 In this limit, the various integrals can be evaluated analytically.
 145 The self-consistency equations (which one is to solve for μ and
 146 \mathcal{N}) become

$$147 \Lambda(0, H) = \left(\frac{\sigma^2}{2\pi}\right) \left[\frac{\mu}{\mu^2 - \mathcal{N}^2}\right] \quad [S5]$$

$$148 \mathcal{N} = 2\Delta \left(\frac{\sigma^2}{2\pi}\right) \left[\frac{\mathcal{N}}{\mu^2 - \mathcal{N}^2}\right]$$

149 from which it follows that the critical value of Λ for the
 150 occurrence of the nematic phase is

$$151 \Lambda_c = \frac{\sigma}{2\sqrt{\pi}\Delta}. \quad [S6]$$

152 For $\Lambda < \Lambda_c$, $\mu = \sigma^2/2\pi\Lambda$ and the in-plane correlation lengths
 153 and intensities of the peaks at \vec{Q}_x and \vec{Q}_y are

$$154 \xi_{ab}(\vec{Q}_x) = \xi_{ab}(\vec{Q}_y) = \frac{1}{\sqrt{\mu}} \quad \text{and}$$

$$155 S(\vec{Q}_x) = S(\vec{Q}_y) = 2\pi\Lambda|\xi_{ab}(\vec{Q}_y)|^4.$$

156 For $\Lambda > \Lambda_c$, $\mu = 2\Delta\Lambda$, $\mathcal{N} = 2\Delta\sqrt{[\Lambda^2 - \Lambda_c^2]}$, and

$$157 \xi_{ab}(\vec{Q}_x) = \frac{1}{\sqrt{\mu + \mathcal{N}}}, \quad \xi_{ab}(\vec{Q}_y) = \frac{1}{\sqrt{\mu - \mathcal{N}}}, \quad [S7]$$

158 and

$$159 \frac{S(\vec{Q}_y)}{S(\vec{Q}_x)} = \left[\frac{\xi_{ab}(\vec{Q}_y)}{\xi_{ab}(\vec{Q}_x)}\right]^4. \quad [S8]$$

160 To address the growth of 3D correlations in the nematic
 161 phase, it is obviously necessary to include explicitly the effects
 162 of non-zero V_z . While the self consistency equations are still
 163 analytically tractable, the solutions are sufficiently complicated
 164 that we only evaluate them numerically. The inter-plane
 165 correlation length can be computed as

$$166 \xi_c = (c/2) \left[\text{arcsinh}(1/\xi_{ab}\sqrt{2V_z})\right]^{-1}. \quad [S9]$$

167 Clearly, there is strong tendency to increased 3D order when
 168 the in-plane correlations become sufficiently long.

169 In Fig. S1, we show the evolution of these quantities
 170 computed numerically from the full self-consistency equations
 171 with $V_z = 0.1$ as a function of Λ for two different values

172 of σ , one representative of the More and one of the Less
 173 disordered regimes, under the assumption $\sigma_{\text{More}}/\sigma_{\text{Less}} = 1.5$.
 174 To make contact with experiment, one should imagine that
 175 the field dependence of Λ determined by competition with
 176 superconductivity, $\Lambda = \Lambda_0[1 - |\phi|^2]$, where the amplitude of
 177 the superconducting order ϕ is (presumably) a decreasing
 178 function of increasing H . There is clearly a sharp increase in
 179 the in-plane correlation lengths and peak intensities at the
 180 nematic phase transition.

181 **Subtleties and ambiguities:** One implication of “random-
 182 field-type” disorder is slow dynamics which inevitably result in
 183 the system falling out of equilibrium upon cooling before the
 184 point of the transition is reached. A rather subtle experimental
 185 protocol is necessary to establish the existence of a broken
 186 symmetry phase experimentally [S4]. However, YBCO is
 187 weakly orthorhombic, which in the current context means
 188 that there is effectively always a small symmetry breaking
 189 field; this rounds the transition to the nematic state, but
 190 at the same time reduces the tendency to the formation of a
 191 metastable nematic domain structure. (From a complementary
 192 perspective, it is possible to look for a growing thermodynamic
 193 correlation length by detecting [S5] the telltale hysteresis and
 194 noise characteristic of the random-field-Ising model in this
 195 limit [S6].)

196 One might still worry that the time-scales involved in a
 197 pulsed field experiment could exacerbate non-equilibrium ef-
 198 fects. However, since the slow dynamics are associated with
 199 reorientation of growing domains [S7, S8], the characteristic
 200 relaxation rates depend exponentially on domain size. There-
 201 fore, once the experimental time scales are large compared to
 202 microscopic time scales (as they are in our experiment), an
 203 enormous increase in the time scale only permits one to probe
 204 the equilibrium physics of slightly larger domains.

205 Finally, it is tempting to try to estimate the volume frac-
 206 tions of the More and Less disordered regions from the relative
 207 strengths of their contributions to the x-ray scattering inten-
 208 sity, $I(\vec{k})$. However, making connection between the calculated
 209 and measured quantities carries with additional uncertainties.
 210 $I(\vec{k})$ is generally dominated by scattering of the atomic cores,
 211 and so is a measure of the atomic displacements. A periodic
 212 pattern of atomic displacements proportional to the CDW
 213 order parameter, ψ , is generic. However, while positions and
 214 widths of the observable peaks in $I(\vec{k})$ reflect the pattern
 215 of translation symmetry breaking and the CDW correlation
 216 length, the variation of intensity from one Brillouin zone to the
 217 other encodes the precise pattern of induced lattice distortion.
 218 Crudely,

$$219 I(\vec{k}) = I(\vec{K} + \vec{Q}) \approx I_0(\vec{K})S(\vec{Q}) \quad [S10]$$

220 where \vec{K} is a reciprocal lattice vector, and $I_0(K)$ is a compli-
 221 cated structure factor.

222 If the scattering intensities were measured in sufficiently
 223 many different Brillouin zones, one could work backwards to
 224 the actual lattice displacements induced by the CDW. This
 225 has been undertaken for the low field diffraction data in Ref.
 226 [S9]. Because of the constraints of the high field experiment,
 227 our data is limited to little over one Brillouin zone, so such
 228 a refinement is not possible. Even in the one Brillouin zone
 229 we study, we have not directly measured the peak width in all
 230 directions — our estimates of the correlation volume involve
 231 the implicit assumption that the correlation length is not much
 232 different in the a and b directions. For all these reasons, there

249	is considerable unavoidable uncertainty in any estimate we	we find the integrated intensity in the 2D peaks is roughly 5	311
250	might make of the relative volume fractions of the two regions.	times that in the 3D peak suggesting that something between	312
251	These worries aside, in the ortho-VIII sample at 25 T [S10],	10% and 20% of the sample is Less disordered.	313
252			314
253			315
254			316
255	S1 Nie L, Tarjus G, Kivelson SA (2014) Quenched disorder and vestigial nematicity in the pseudo-gap regime of the cuprates. <i>PNAS</i> 111(22):7980–7985.	derdoped $\text{YBa}_2\text{Cu}_2\text{O}_{7-\delta}$ Nanowires: Evidence for Fluctuating Domain Structures. <i>Phys. Rev. Lett.</i> 93(8):087002.	317
256	S2 Nie L, Sierens LEH, Melko RG, Sachdev S, Kivelson SA (2015) Fluctuating orders and quenched randomness in the cuprates. <i>Phys. Rev. B</i> 92(17):174505.	S6 Carlson EW, Dahmen KA, Fradkin E, Kivelson SA (2006) Hysteresis and Noise from Electronic Nematicity in High-Temperature Superconductors. <i>Phys. Rev. Lett.</i> 96(9):097003.	318
257	S3 (Note) Strictly speaking, the nematic phase we find for $V_z = 0$ is an artifact of the large N approximation; random field disorder precludes even discrete symmetry breaking in 2D. However, as shown in ref. [1], for small but non-zero V_z , the nematic phase is robustly recovered, even when V_z is small enough that it has little effect on the quantities considered here.	S7 Bruinsma R, Aeppli G (1984) Interface Motion and Nonequilibrium Properties of the Random-Field Ising Model. <i>Phys. Rev. Lett.</i> 52(17):1547–1550.	319
258		S8 Huse DA, Fisher DS (1987) Dynamics of droplet fluctuations in pure and random Ising systems. <i>Phys. Rev. B</i> 35(13):6841–6846.	320
259		S9 Forgan EM et al. (2015) The microscopic structure of charge density waves in underdoped $\text{YBa}_2\text{Cu}_3\text{O}_{6.54}$ revealed by X-ray diffraction. <i>Nat Commun</i> 6:10064.	321
260	S4 Birgeneau RJ, Shapira Y, Shirane G, Cowley RA, Yoshizawa H (1986) Random fields and phase transitions. <i>Physica B+C</i> 137(1):83–95.	S10 Gerber S et al. (2015) Three-dimensional charge density wave order in $\text{YBa}_2\text{Cu}_3\text{O}_{6.67}$ at high magnetic fields. <i>Science</i> 350(6263):949–952.	322
261	S5 Bonetti JA, Caplan DS, Van Harlingen DJ, Weissman MB (2004) Electronic Transport in Un-		323
262			324
263			325
264			326
265			327
266			328
267			329
268			330
269			331
270			332
271			333
272			334
273			335
274			336
275			337
276			338
277			339
278			340
279			341
280			342
281			343
282			344
283			345
284			346
285			347
286			348
287			349
288			350
289			351
290			352
291			353
292			354
293			355
294			356
295			357
296			358
297			359
298			360
299			361
300			362
301			363
302			364
303			365
304			366
305			367
306			368
307			369
308			370
309			371
310			372

DRAFT

373
374
375
376
377
378
379
380
381
382
383
384
385
386
387
388
389
390
391
392
393
394
395
396
397
398
399
400
401
402
403
404
405
406
407
408
409
410
411
412
413
414
415
416
417
418
419
420
421
422
423
424
425
426
427
428
429
430
431
432
433
434

435
436
437
438
439
440
441
442
443
444
445
446
447
448
449
450
451
452
453
454
455
456
457
458
459
460
461
462
463
464
465
466
467
468
469
470
471
472
473
474
475
476
477
478
479
480
481
482
483
484
485
486
487
488
489
490
491
492
493
494
495
496

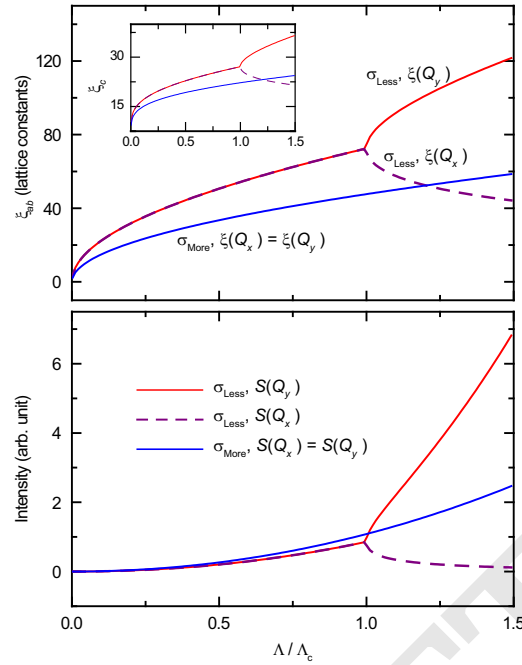


Fig. S1. Correlation lengths (upper panel) and peak intensities (lower panel) associated with the x and y directed components of the CDW order parameter as a function of increasing mean squared magnitude of the local CDW order parameter for the “Less” and “More” disordered regions. We have taken $\sigma_{\text{More}} = 1.5\sigma_{\text{Less}}$, $V_z = 0.1$, and for graphical clarity have rescaled S for the More disordered regions by a factor of 3. The main panel a shows the in-plane correlation lengths, while the inset shows the correlation length with the z -direction (e.g., c -axis). Here, Λ_c is the critical value of the CDW magnitude in the Less disordered regions, and for simplicity we show results for $T = 0$. $\xi_{ab}(\mathbf{Q})$ and $\xi_c(\mathbf{Q})$ are the in-plane and out-of-plane correlation lengths corresponding to ordering vector \mathbf{Q} , respectively.

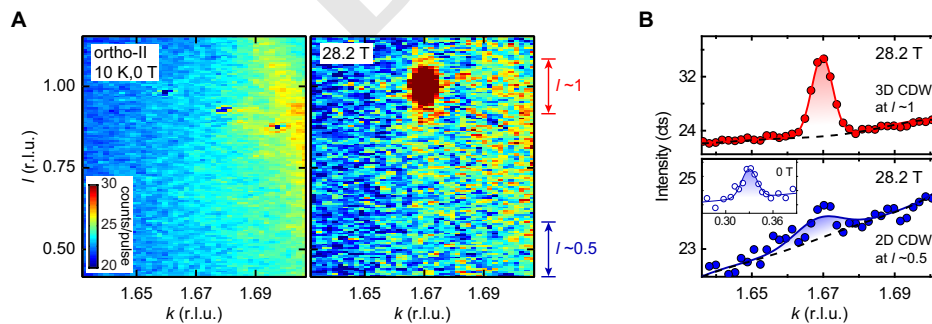


Fig. S2. (A) Diffraction intensity of ortho-II in the kl -plane near $(0, 2-q, 1)$ at zero magnetic field (left panel) and at high magnetic field (right panel). Note that the feature around $k \sim 1.7$ and $l \sim 0.8$ is a condensation of water molecules results in the formation of an “ice ring” in the vicinity of the CDW signal [S10]. (B) Projected intensities from the diffraction pattern at $\mu_0 H = 28.2$ T near $l \sim 1$ (upper panel) and $l \sim 0.5$ (lower panel). It indicates the coexistence of 3D and quasi-2D CDW orders in YBCO ortho-II under the high magnetic field. Inset (RSXS data) shows the quasi-2D CDW orders in YBCO ortho-II at $\mu_0 H = 0$ T and $T \sim 20$ K. Colored solid lines are Gaussian fits to the high-field data with polynomial backgrounds at zero-field (black dashed line).

497
498
499
500
501
502
503
504
505
506
507
508
509
510
511
512
513
514
515
516
517
518
519
520
521
522
523
524
525
526
527
528
529
530
531
532
533
534
535
536
537
538
539
540
541
542
543
544
545
546
547
548
549
550
551
552
553
554
555
556
557
558

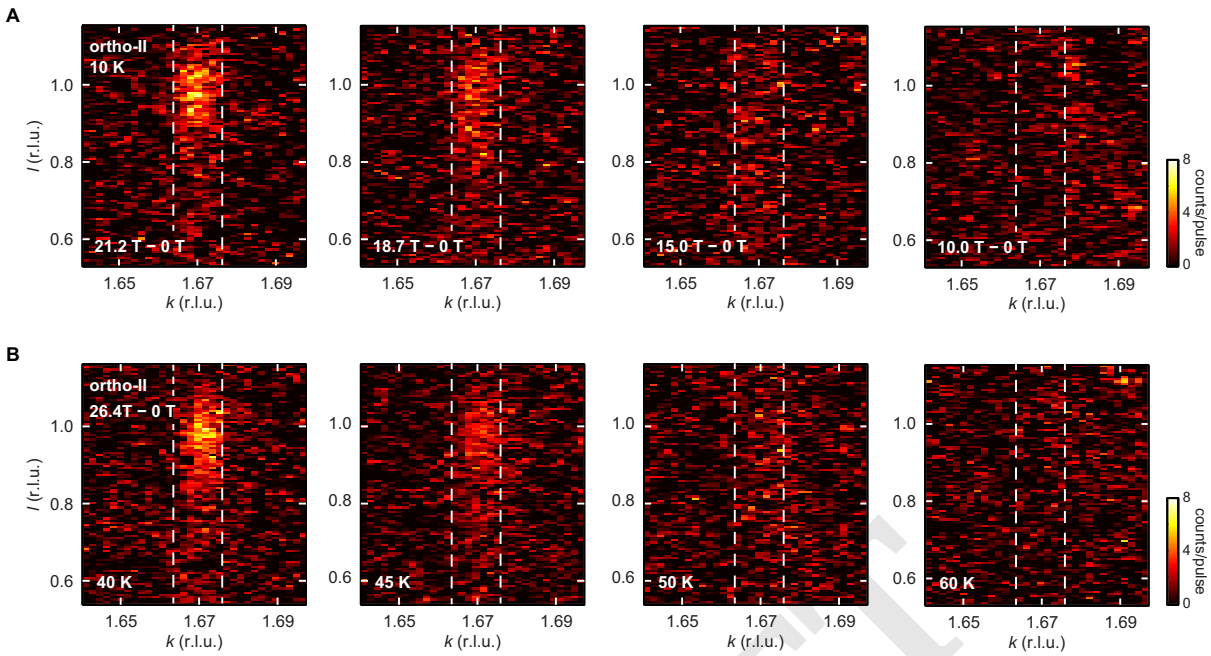


Fig. S3. (A) Magnetic field dependencies. (B) Temperature dependencies. Dashed lines indicate the windows used to deduce the projected peak profiles of Figs. 2A and 2D in the main text.

559
560
561
562
563
564
565
566
567
568
569
570
571
572
573
574
575
576
577
578
579
580
581
582
583
584
585
586
587
588
589
590
591
592
593
594
595
596
597
598
599
600
601
602
603
604
605
606
607
608
609
610
611
612
613
614
615
616
617
618
619
620

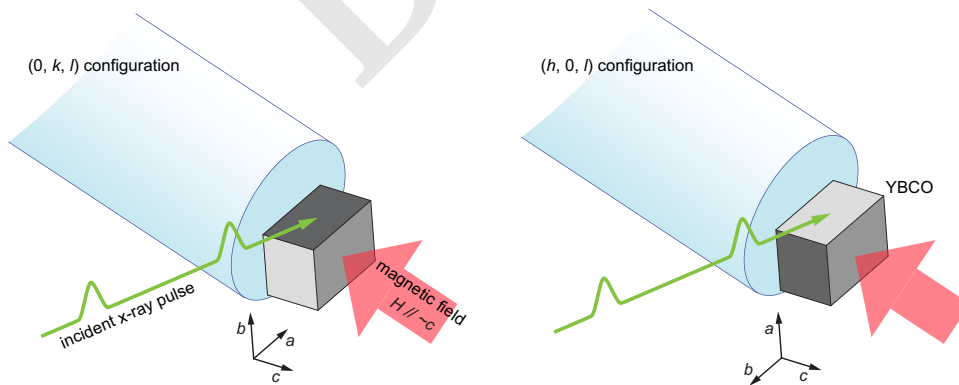


Fig. S4. Crystallographic orientations of YBCO crystals used for the measurement of the $(0, k, l)$ reflection (left) and $(h, 0, l)$ reflection (right). The green line represents the incident x-ray free electron pulses. The red arrow indicates the direction of the magnetic field.